NOx emissions estimation methodology for air-breathing reusable access to space vehicle in conceptual design

Acta Astronautica 216 (2024) 304–317

Contents lists available at ScienceDirect

Acta Astronautica

journal homepage: www.elsevier.com/locate/actaastro

NOx emissions estimation methodology for air-breathing reusable access to space vehicle in conceptual design

Roberta Fusaro [a,*], Guido Saccone [b], Nicole Viola [a]

[a] Department of Mechanical and Aerospace Engineering, Politecnico di Torino, Corso Duca Degli Abruzzi 24, 10129, Turin, Italy

[b] Propulsion and Space Exploration Technologies Unit, Italian Aerospace Research Centre - CIRA, Via Maiorise Snc, 81043, Capua, (CE), Italy

ARTICLE INFO

Keywords:
Reusable launchers
Air-breathing propulsive technologies
Nitrogen oxides emission estimation
Synergetic air-breathing rocket engine
Skylon
$P3T_3$method

ABSTRACT

With an expected global revenue exceeding 1 trillion USD by 2040, the space industry is one of the world's fastest-growing sectors. Given the booming investment in the space industry and the anticipated space tourism era, it is crucial to assess the impact of already operative launch assets as well as to adopt design-to-sustainability strategies for the under-development and future launchers. This paper discloses an integrated methodology to estimate nitrogen oxides emissions of a hydrogen-fuelled air-breathing concept. The proposed strategy combines multi-fidelity propulsive system modelling with 0D chemical-kinetic air/hydrogen combustion numerical simulations to define a high-fidelity emissive database representative of various on-ground and in-flight operative conditions. The propulsive and emissive databases are then used to suggest an analytical formulation able to predict nitrogen oxides emission indices in any in-flight conditions, perfectly fitting the conceptual design needs. Throughout the paper, the Skylon spaceplane and its Synergetic Air Breathing Rocket Engine are used as case study. The methodology disclosed allows proving the high competitiveness of this air-breathing space launchers with respect to famous past and current competitors, as the Space Shuttle and the Falcon 9.

1. Introduction

With an expected global revenue exceeding 1 trillion USD by 2040 [1,2] the space industry is one of the world's fastest-growing sectors. Given the booming investment in the space industry and the anticipated space tourism era, it is crucial to assess the impact of already operative launch assets as well as to adopt design-to-sustainability strategies for the under-development and future launchers [3]. Space technologies are valuable assets for environmental protection and can support the United Nation's (UN) Sustainable Development Goals (SDG) on Earth, but these technologies do also have environmental impacts. Recent policy has focused on space debris, the in-space pollution that satellites, launchers and space systems produce in orbit. While orbital debris may well be viewed as the most consequential threat from current space activities, the appropriate scope to understand the full environmental cost of the expanding space industry shall also encompass ground and atmospheric consequences [4]. While the scientific understanding is limited, studies suggest that the impact of rocket emissions will continue growing with increased launches and may reach unsustainable levels [3]. Nowadays, the contribution of space launch activities to the radiative factor (RF) equals 16 ± 8 mW m^{-2} [5]. Traditional launchers consume $\sim 4 \bullet 10^4$ t of propellant [5] annually versus $2 \bullet 10^8$ t of kerosene for the aviation sector. Therefore, burning $\sim$0.01 % of the fuel (or propellant) that global aviation consumes, rockets are considered small contributors to the environmental impact of the transportation sector. However, depending on the chemical composition of the propellant used, rocket engines can emit up to more than a hundred times more soot than modern turbine engines, on an emission index (EI) basis [6]. Moreover, subsonic aircraft release most of their exhaust into the upper troposphere, where the lifetime of the different species varies from days to several months [7,8], whilst rockets mostly entirely emit exhaust above the tropopause, where the lifetime of combustion products is of 3–5 years [9], with a serious potential risk of particles accumulation [10,11].

Complementary, the fast-growing request to access to space is pushing the research activities of the aerospace sector to develop breakthrough technologies and innovative products capable to meet design-to-sustainability strategies. Within this context, reusable access to space vehicles are gaining more and more attention. Among those systems, spaceplanes take-off and land horizontally, thus combining lift and thrust forces and exploiting existing airport infrastructures. Spaceplanes employ air-breathing engines up to the stratosphere and, then, rocket engines to reach the target orbit. The latest evolutions of multidisciplinary design approaches combined with agile design

* Corresponding author.
E-mail addresses: roberta.fusaro@polito.it (R. Fusaro), g.saccone@cira.it (G. Saccone), nicole.viola@polito.it (N. Viola).

https://doi.org/10.1016/j.actaastro.2023.12.060
Received 22 August 2023; Received in revised form 14 December 2023; Accepted 31 December 2023
Available online 7 January 2024

Nomenclature

P_3	Pressure at the inlet of the combustion chamber
T_3	Temperature at the inlet of the combustion chamber
H	Air humidity factor

Acronyms/Abbreviations

Al2O3	Aluminum Oxide
BC	Black Carbon
CC	Combustion Chamber
Clx	Chlorine
CO	Carbon monoxide
CO2	Carbon dioxide
EDB	Emission DataBase
EI	Emission Index
FAA	Federal Aviation Administration
FAR	Fuel to Air Ratio
FL	Flight Level
GHG	GreenHouse Gases
H2O	Water Vapour
H2–P3T3	Hydrogen and High-speed P3T3 formulation
HX	Heat Exchanger
ICAO	International Civil Aviation Organization
LEO	Low Earth Orbits
NOx	Nitrogen Oxides
PB	Preburner
REL	Reaction Engines Limited
SABRE	Synergetic Air Breathing Rocket Engine
SDG	Sustainable Development Goals
SL	Sea level
UN	United Nation
USD	United States Dollars

methodologies and the recent advancements in computational resources have already reduced the time for the conceptual design of these very complex aerospace systems. However, it is only by implementing a complete holistic design framework that engineers can dramatically reduce the risk of developing unsuccessful products, checking the sustainability of the concept (from the economic [12], technological [13] and environmental perspectives) since the conceptual design stage. In fact, the methodology shall be able to properly capture the various design factors that directly affect the amount, the type, and the effect of the released exhausts, including the class of launcher, the type of propellant, the specific propulsive technology, as well as peculiar aspects of the concept of operations such as mission profile and staging strategy, etc.

In this complex and very challenging scenario, this paper aims at suggesting how to anticipate pollutant and Green House Gases (GHG) emissions prediction for reusable access to space vehicle since the conceptual design phase, specifically focusing on nitrogen oxides emissions. To unlock the possibility to anticipate the environmental sustainability assessment, the authors couple simplified but accurate propulsive systems models with 0D chemical-kinetic combustion models (see Fig. 1). Obviously, to make these models useful for the conceptual design stage, they shall require a minimum set of input data (in line with the information usually available at this stage) and minimal computational resources (to be compatible with the fast design loops). Moreover, they shall be highly reliable (to support decisions with very high committed costs).

The paper starts from reporting on the state of the art in emissions modelling for aerospace applications (Section 2). Here, an analytical model, originally developed for the aeronautical sector is selected as the most promising baseline to be further upgraded and extended, thus guaranteeing the applicability to future reusable access to space vehicles. To achieve this goal, a step-by-step methodology is disclosed (Section 4) and the Skylon launcher with its SABRE engine (Section 3) is used as case study throughout the paper. The suggested methodology is one of the innovative elements of this paper: it consists of three main steps: the definition of a multi-fidelity propulsive model and the consequent definition of a propulsive database (Section 4.1), the development of a 0D chemical-kinetic combustion model and the consequent development of a high-fidelity chemical emission database (Section 4.2) and the exploitation of the propulsive and emissive databases for the development of a new analytical formulation for NOx prediction in conceptual design (Section 4.3). The application of the

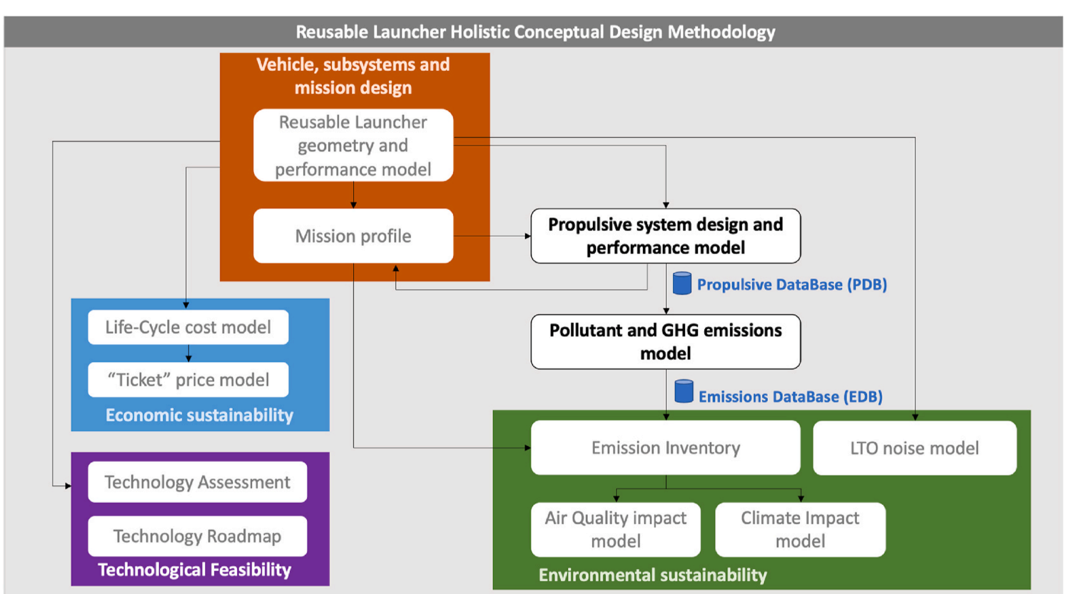

Fig. 1. Reusable Launcher holistic design approach.

entire methodology flow to the Skylon vehicle (in Section 5) reveals the uttermost advantage in terms of environmental impact of this reusable launcher solution with respect to conventional expendable launchers (Section 5).

Eventually, to better guide the reader through this paper, it might be worth briefly highlighting the main innovative aspects of each of the following sections.

- Section 2: for the first time, a comprehensive review discusses the applicability of the existing emission modelling techniques to space launchers. The lack of existence of a quick but reliable estimate of chemical emissions of space launchers during its atmospheric ascent urges the exploitation of high-fidelity data to build semiempirical models and new analytical formulations.
- Section 3: the SABRE engine selected as case-study perfectly shows the high-level of complexity of the propulsive system of a future space launcher.
- Section 4: the methodology contains several elements of innovation: (i) the methodology implements a multi-fidelity approach to generate the emission dataset necessary to develop the new analytical correlation; (ii) a complete thermodynamic model of the SABRE engine in its air-breathing mode of operation is disclosed; (iii) for the first time, 0D chemical-kinetic investigations of the SABRE engine are reported for the entire range of Mach numbers (up to Mach 5) experienced by the vehicle in its atmospheric ascent; (iv) the H2–P_3T_3, the Hydrogen and High-speed P_3T_3 formulation is disclosed, making the method applicable, for the first time, to high-speed vehicles using hydrogen as fuel.
- Section 5: the developed methodology and the newly disclosed formulation allows comparing, for the first time, already existing launchers and future reusable launchers in terms of chemical emissions during the atmospheric phase, revealing the uttermost advantage in terms of environmental impact of the future reusable launcher solution.

2. State of the art in emissions modelling for aerospace applications

When it comes to environmental impact, the aviation sector is considered a hard-to-abate sector, together with the maritime transport sector and several industrial activities, including steel and cement production. Thus, in the last decade, there has been a booming investment from the public and private sectors in funding fundamental research, technology development, and proof-of-concepts to envisage a greener future for the next generation of aircraft. A different scenario can be depicted for space activities, where the attention has been focused on reducing the space-debris problem at first, and only very recently, the sustainability of the launch sector has emerged. Therefore, the literature reports still very few attemptsto estimate chemical emissions for space launchers. In Ref. [14], the licensing of new space launchers is addressed. The Federal Aviation Administration (FAA) requires all new launch vehicles and spaceports to acquire operator licenses. This licensing process imposed by the Federal Aviation Administration (FAA) involves an environmental review to assess the potential impacts of rocket emissions. However, no standard procedure for estimating rocket emissions currently exists and the authors generate a database of emissions indices using a NASA-developed software compared with previous estimates. The most detailed emissions results that are publicly available in the literature refer to the Space Shuttle and other historical NASA launch vehicles [15–24]. Although these set of data is not representative of the state-of-the-art propulsive technologies, they can be very useful as a base for the development of semi-empirical models able to capture the differences due to the type of propellant. Conversely, looking at the most recent progresses, Larson et al. [25] performed a unique study to estimate the global atmospheric response to emissions of reusable access to space vehicles, namely, the Skylon vehicle. However, the NOx estimation model used in this publication is purely based on a stochiometric reaction, neglecting initialization, branching, chain propagation, and termination mechanisms which have been experimentally demonstrated to be highly important for the correct prediction of NOx formation in the H_2-air combustion process [26]. In this context, the present paper discloses new analytical formulations able to support the NOx prediction of future space launchers with a more robust and reliable emission database. A 0D chemical-kinetic model has been set up and used (Section 4.2) to correctly simulate the hydrogen combustion mechanism and, finally, build a reliable emission database.

Widening the scope of the literature review to the aviation sector, a few examples of analytical formulation for NOx prediction are found. According to Ref. [27], techniques to assess NOx can be classified in a systematic way as 1) correlation-based models, 2) the P_3-T_3 method, 3) fuel flow models, 4) simplified physics-based models, and 5) high-fidelity simulations. Of the simple prediction methods, the most dependable and widely used is the P_3-T_3 method, where the Emission Index (EI) measured at ground level is corrected to the actual in-flight conditions at altitude by using both altitude ground-level combustor operating environments. It is worth remembering that the original P_3-T_3 method is applicable to turbofan engines using traditional jet-fuels (kerosene-based) only. In detail, the estimation methodology is organized according to the following steps (summarized in Fig. 2).

1) the sea-level combustor inlet conditions in terms of pressure (P_{3SL}), temperature (T_3) and fuel-to-air ratio (FAR_{SL}) corresponding to the four throttle settings prescribed in Ref. [28] shall be estimated or retrieved from engine manufacturer's proprietary information. Complementary, NOx emission indexes at sea-level condition ($EINOx_{SL}$) are retrieved from the ICAO Aircraft Engine Emissions Databank. P_{3SL}, FAR_{SL} and $EINO_{SL}$ are plotted against T_3 value corresponding to the four throttle settings.
2) In-flight combustor inlet conditions (P_{3FL}, T_{3FL}, FAR_{FL}) are usually retrieved from manufacturer proprietary data or in case of data unavailability, they can be estimated thanks to accurate and high-fidelity propulsive models.
3) Starting from the in-flight combustor inlet conditions (P_{3FL}, T_{3FL}), the values of P_{3SL}, FAR_{SL} and $EINO_{SL}$, corresponding to combustor inlet temperature at altitude are obtained from the previously mentioned plots.
4) $EINOx_{FL}$ can be determined by using corrective factors accounting for the differences between sea-level and in-flight altitude conditions, according to the following formulation:

$$EINO_{x_{FL}} = EINO_{xSL}\left(\frac{P_{3FL}}{P_{3_{SL}}}\right)^{n}\left(\frac{FAR_{FL}}{FAR_{SL}}\right)^{m} e^{H} \tag{1}$$

Where H is the relative humidity corrective factor [27]. In Ref. [27], it is observed that pressure exponent n of 0.4 and FAR exponent m of zero are the most suitable in case the engine-specific exponents are not known. It is therefore evident that the most impacting parameter on NOx production appears to be the pressure at the beginning of the combustion process, while the fuel-to-air ratio can be neglected.

However, the direct application of this method to the airbreathing engines of a future reusable launcher (as the SABRE mounted on the Skylon) is hampered by the following main reasons.

- The unavailability of data from the ICAO aircraft engine emissions databank for under-development or future engines. In this paper, the authors tackle this issue by coupling the propulsive thermodynamic model of the new engine (i.e. SABRE) with a set of 0D chemical-kinetic simulations. This allows to model and simulate sea-level conditions of the combustor to obtain the set of $EINO_{SL}$.
- The demonstrated validity of the model for subsonic engines using conventional fuels. In this paper, the authors tackle this issue by exploiting the results of the 0D chemical-kinetic simulations to

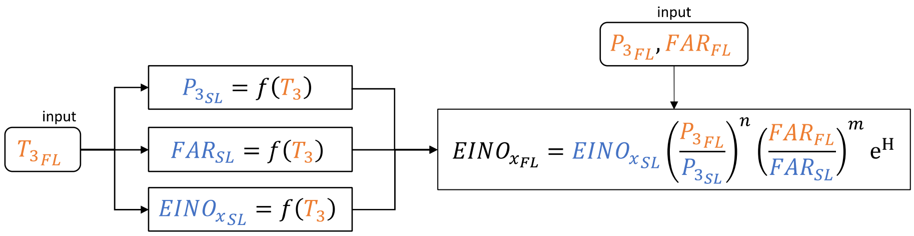

Fig. 2. Original P_3T_3 workflow.

upgrade the analytical formulation (Eq. (1)), thus extending its applicability to hydrogen-fuelled engines able to operate from the subsonic speed regime to the supersonic and hypersonic ones.

3. The Skylon project and its SABRE engine

A spaceplane concept operating an air-breathing engine during the initial part of the ascent benefits from a reduction of propellant consumption, thus showing increased mission performance, mainly in terms of payload mass or delivery altitude. According to Ref. [29], since the advent of high-speed propulsion technology, various combined-cycle engines with dual-mode operations have been proposed to support future spaceplanes missions. An example is the ATREX engine specifically developed to support the initial air-breathing acceleration phase [29–31] of future air-breathing launchers A different approach has been followed by Reaction Engines Limited (REL), whose Skylon spaceplane combines the advantages of an initial air-breathing phase followed by a final rocket phase, integrated in a single engine, namely the SABRE [32,33,34], Synergetic Air Breathing Rocket Engine. The Skylon concept is a reusable single-stage launcher to orbit of about 325 t, able to take-off horizontally from an airport runway, exploiting two SABRE in air-breathing mode up to 25 km, and then, thanks to the same engines operating in rocket mode, it can reach Low Earth Orbits (LEO) to deliver up to 15 t of payload. Finally, the SABRE in air-breathing mode can be exploited again at the end of the mission to complete a runway landing.

Looking at the cutaway reported in Fig. 3, when the SABRE operates in air-breathing mode, the atmospheric air is compressed and injected into the thrust chamber. As the high-speed flight (up to Mach 5 at 25 km of altitude) generates very high intake recovery temperatures (about 1400 K at Mach 5), the air-compressor inlet temperature has to be decreased by means of a pre-cooler (Heat Exchanger HX1 and HX2), which is considered a key-enabling technology of this engine. It is made up of a brazed microchannel built-in Inconel 718, through which the helium flows and cools down 400 kg/s of air of more than 1000 K [35]. The picked-up heat is used to drive the air turbo compressor by means of an intermediate cycle that exploits the helium flowing between the precooler and the cryogenic hydrogen feedline. The thermal power input through the precooler thus not suffice the combustor requirements, thus the combustion process is split into two main sections: a preburner (PB) that provides the additional heat power required and a thrust chamber. A reheater (HX3) heats up the helium stream benefitting of the PB exhausts, which, oxygen rich, are eventually burnt in the main thrust chamber. The He stream that exhausts the turbine is further cooled down through the regenerator (HX4) and then re-compressed with the circulator to supply the pre-cooler. The hot stream of hydrogen which leaves the regenerator drives the liquid hydrogen pump and the circulator. Moreover, it is worth noticing that to deal with high Mach numbers, the excess of air captured by the air intake with respect to the compressor demand is diverted towards a spillage duct and burnt with hydrogen in dedicated by-pass ramjet burners. The air-breathing regime extends from take-off to flight at Mach 5 and 25 km of altitude, a regime at which SABRE transitions to rocket mode for further acceleration to orbital speeds. During rocket operation, the intake is closed, the precooler shuts down and the preburner is the sole power input of the cycle. The onboard oxygen replaces the atmospheric air-supply and the helium stream drives the liquid oxygen turbopump instead of the air turbo-compressor.

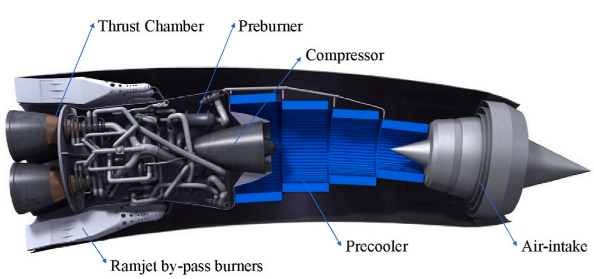

Fig. 3. Synergetic Air Breathing Rocket Engine cutaway. Readapted from [36].

4. Methodology

The main objective of this paper is to disclose an ad-hoc developed analytical formulation, namely H2–P_3T_3, able to anticipate the environmental sustainability assessment of a reusable launcher at the very beginning of the design process. As highlighted in Fig. 1 and summarized in Section 1, to achieve this goal and to allow for the application of the P3-T3 method, it is essential to develop parametric propulsive and emission models able to capture the peculiarities of reusable launchers in a simple and reliable way. Specifically, in order to better fit the conceptual design stage, thus avoiding the need for high-fidelity numerical simulations, the propulsive model is developed following an analytical approach. In detail, combining a parametric cycle analysis with a performance cycle analysis, the model is able to generate a preliminary propulsive database collecting the variation of thrust, specific fuel consumption, fuel-to-air ratios, temperature and pressure conditions at the entrance of the combustion chamber throughout the reference mission. This set of data is essential to feed the emission model which makes use of analytical formulations to predict the emission indexes for the most important pollutant and GHG species, contributing to the build-up of the first Emission DataBase (EDB). Then, thanks to the connection with the mission profile, an emission inventory can be compiled.

In the next subsections, details on both the propulsive system model and the emission model are reported together with the details of the application of the methodology to the SABRE engine.

4.1. Propulsive system modelling

As graphically depicted in Fig. 4, the propulsive system design and performance model directly follows a first design loop at the vehicle and mission level aimed at defining a first minimum set of requirements (mainly, functional, configurational, performance and mission requirements). Specifically, the subset of requirements allocated onto the propulsive system shall guide the very first step of this approach, which consists of the identification of the main constituent components of the engine. Once the basic "bricks" are identified, two main activities can be run in parallel: on the one hand, it is possible to consider each

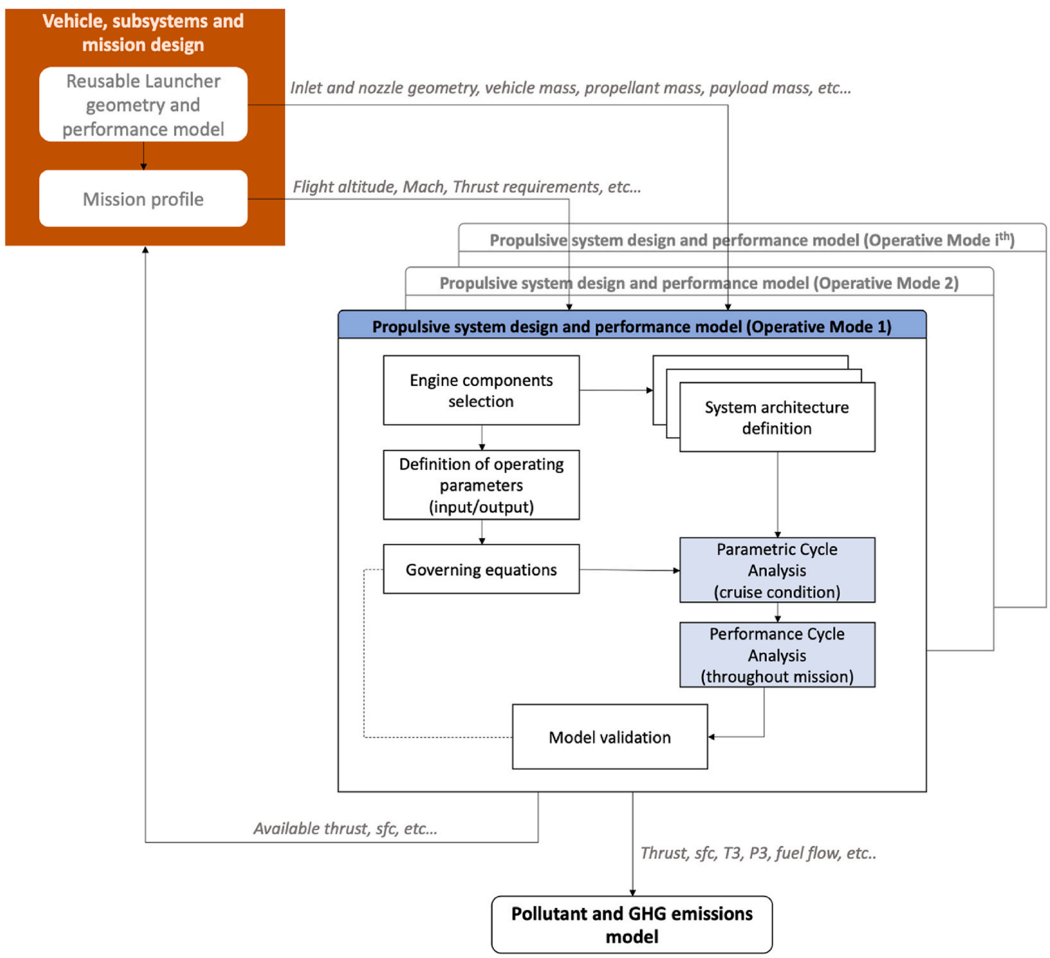

Fig. 4. Propulsive system modelling activity flow.

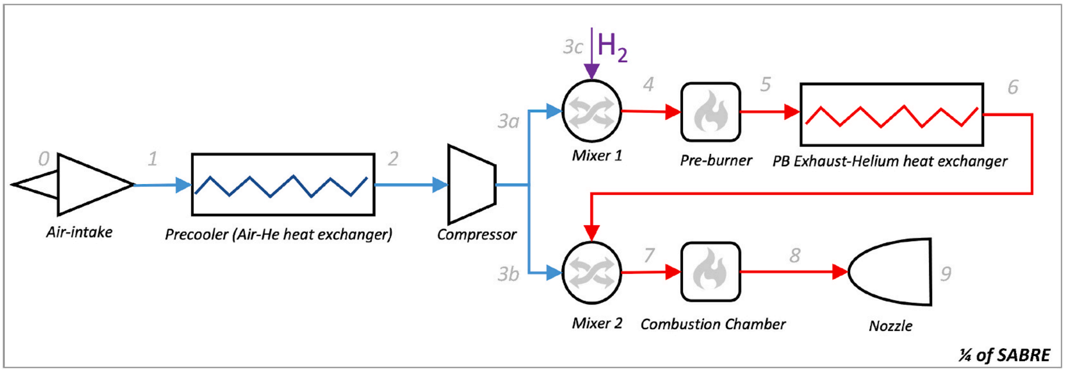

Fig. 5. One-fourth of the SABRE propulsive model.

component as black box, mainly focusing on the input/output variables per each of them; on the other hand, the set of identified engine components can be combined in several different ways to better mimic the desired engine architecture. This last step is crucial to anticipate propulsion system design and performance modelling at the conceptual design stage. In fact, the possibility of dealing with multiple systems architectures gives the designers the opportunity of implementing a sort of multi-fidelity approach, representing the same engine with a combination of components with increasing complexity. Once the input/output variables have been identified, it is necessary to describe each "black box" with its set of governing equations, to eventually enable the core analyses of this model: the parametric cycle analysis and the performance cycle analysis. In line with [37], the main objective of parametric cycle analysis is to obtain estimates of the performance parameters (primarily specific thrust and thrust specific fuel consumption) in terms of design limitations (such as maximum allowable turbine temperature and attainable component efficiencies), and design choices (such as compressor pressure ratio, fan pressure ratio, bypass ratio, and theta break) in specific flight conditions. The comparative simplicity of the aerothermodynamic analysis is achieved by treating each stream as one-dimensional flow of a perfect gas, by representing non-ideal component behaviour through realistic efficiencies. Then, the inclusion of non-ideal (or real) component behaviour to the degree desired leads to a close imitation of nature, even for very complex configurations.

Performance analysis differs significantly from parametric analysis. In parametric (reference or design point) cycle analysis all design choices (including the flight conditions) are free to select by the designer, and the engine performance characteristics per unit mass flow are determined for each selected set of choices. In contrast, in performance cycle analysis the design choices have been made, and the performance of this specific reference point engine is needed at all possible operating conditions. The independent variables in performance analysis are flight conditions, throttle settings, and nozzle settings. Once the engine is sized and the mass flow rate specified, performance analysis is employed to determine how a selected engine performs at all operating conditions within its flight envelope.

At this point, it is important to highlight that reusable launchers projects may be characterised by unprecedented innovations from the propulsive system standpoint. In order to guarantee an adequate level of accuracy of the propulsive performance estimations, a model validation step is mandatory to properly tune the parameters of the governing equations and better represent the real engine behaviour since the conceptual design stage. To support this model validation and refinement activity, results of high-fidelity simulations or test campaigns can be directly exploited. Lastly, to meet their mission objectives, reusable launchers can be equipped with multiple propulsive subsystems or with a single one able to operate in different operating modes. Therefore, it is essential to build dedicated models per each of the expected operating modes of the system.

4.1.1. Propulsive modelling of the SABRE engine

Even if the rocket phase of the SABRE is obviously of extreme importance for the mission of Skylon, the main innovation of the propulsive architecture resides in the air-breathing phase, which is then the most interesting here, while the rocket phase model will be briefly presented later in order to evaluate the overall environmental impact of the engine. Following the methodology reported in the previous subsection, three different models have been developed with an increasing complexity approach, to ensure different alternatives that can be chosen based on the degree of maturity of the design. Only the most complete and reliable model is here reported, discussed and used in the following sections.

Hereafter, the main simplifications of the developed mathematical model are reported.

1) According to Ref. [29], the SABRE engine comprises 4 thrust chambers, 2 preburners-reheater units, 2 hydrogen turbopumps, 2 regenerators and 2 He-circulators driven by a hydrogen turbine. This configuration allows the SABRE to operate as a single air-breathing engine with 4 thrust chambers and as 2 independent rocket engines. This suggests the possibility to simplify the engine propulsive model to ¼ of the real engine, by describing a single unit of each type (Fig. 5). In consequence, thrust and mass flow rates performance obtained with this model are representative of an ideal engine which is one-fourth of the full scale one for what concerns the air-breathing mode of operation.
2) The air-intake is assumed to perform with nominal pressure recovery, perfectly matching the air-compressor demand throughout the air-breathing mission. Thus, the bypass ramjets are neglected.

The main input data used to model and simulate the behaviour of the SABRE throughout its air-breathing mode (Fig. 6) is summarized in Table 1. Details on the air and hydrogen mass flow rates as well as of the pressure and temperature at the air-intake are reported in Fig. 7.

The model has been validated by comparing the estimated thrust output with the available data from the literature [29]. As reported in Fig. 8, the results are in line with the expectations, with errors lower than 6 %.

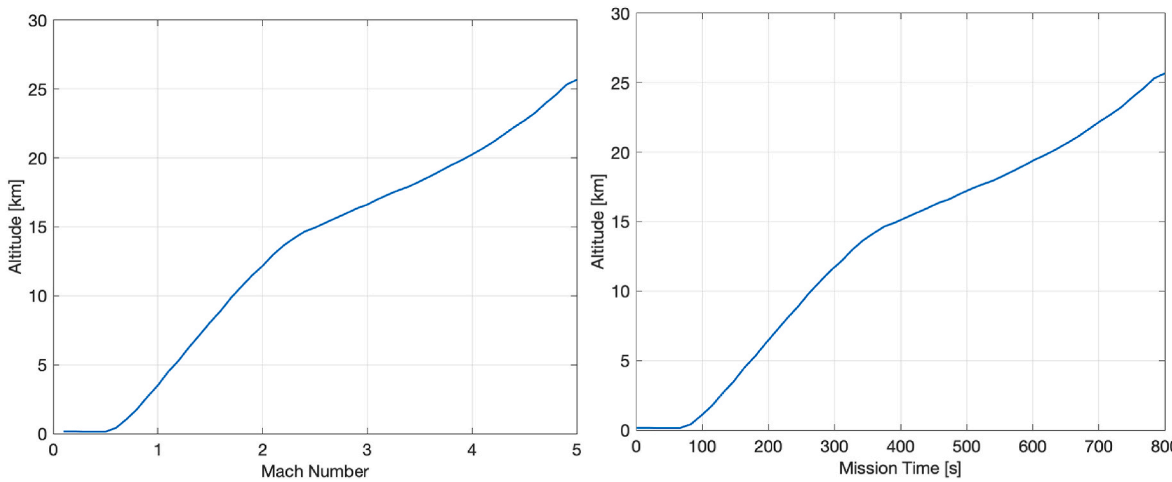

Fig. 6. Skylon mission profile during the air-breathing ascent. a) Altitude profile vs Mach number; b) Altitude profile vs mission time.

Table 1
Input data of the SABRE propulsive model.

	Parameters	Value
Preliminary	*Free stream Mach number*	0–5
	Altitude	0–25000 m
	Air mass flow	77.3–92 kg/s
Intake	*Intake total pressure recovery*	0.15–0.95
Precooler	*PC pneumatic efficiency,*	72 %
	PC outlet temperature,	97 K
Air compressor	*AC efficiency*	0.8
	AC pressure ratio	65–180
Liquid Hydrogen Tank	*fuel/air equivalence ratio*	2.5–2.8
	Tank temperature	18 K
	Tank pressure	1 bar
Liquid Hydrogen Pump	*Efficiency*	0.8
	LHP compression ratio	257
Hydrogen turbine	*Efficiency*	0.8
Helium turbine	*Efficiency*	0.8
	Turbine inlet temperature	1190 K
Helium compressor	*Compressor inlet temperature*	50 K
	Compressor efficiency	0.8
Node CC-PB	$\frac{\dot{m}_{PB}}{\dot{m}_{tot}}$	0.45–0.6
Pre-burner	*Combustion efficiency*	0.9
	Pneumatic efficiency	0.95
	Lower calorific value,	120.9e6 J/kg
Nozzle	*Pneumatic efficiency*	0.98
	Efficiency	0.95
	Area ratio at separation	20–100

4.2. Pollutant and GHG emissions modelling

The second part of the methodology reported in this paper refers to the exploitation of the propulsive model outputs to set up 0D chemical-kinetic simulations to properly estimate nitrogen oxides emission indices (Fig. 9). This is necessary to build a consistent and reliable emissions database to be used as a basis in the third part of this work, to upgrade the analytical equations of the P3-T3 method. In detail, emission indices were approximately estimated using a high-fidelity chemical kinetic method, explained in more detail in Ref. [38], which, however, neglects the fluid-dynamic and turbulence-chemistry interactions actually occurring within the engine's combustion chambers.

Particularly, the mass fractions of the pollutant substances were evaluated through 0D simulations of closed, perfectly stirred, adiabatic batch reactors filled with reacting mixtures corresponding to the same inlet composition, temperature and pressure of several sea levels and flight Mach number conditions, previously determined for both the preburner and the combustion chamber stages.

Cantera is an open-source software for zero-dimensional mathematical-chemical modelling, used in this work under Python interface [39]. It performs 0D time-dependent simulations of homogeneous, isochoric and adiabatic batch reactors with premixed gaseous reacting hydrogen/oxygen mixtures.

For this purpose, the kinetic mechanism by the Z24_NOx20 modelling group was successfully used [40,41].

This is a novel detailed reaction mechanism for hydrogen/air combustion essentially representing an updated version of the previous Z22 kinetic mechanism developed by Zettervall and Fureby [21], with the aim to expand the operating range above 8 atm. It was formulated by the Swedish Research and Defence Agency (FOI) and it is openly available [FOI report]. Z22 is a detailed, hydrogen/oxygen kinetic mechanism consisting of 9 species and 22 irreversible elementary reactions [41].

Zettervall and Fureby [40] highlight the importance of competition in the chain-branching reaction [R4]:

[R4] $H + O_2 \rightarrow OH + O$

and the chain-propagating reaction [R12]:

[R12] $H + O_2\ (+M) \rightarrow HO_2\ (+M)$

The first creates a pool of radical species effectively decreasing the ignition time, while the second produces the hydroperoxyl radical, which inhibits the chain-branching combustion process and therefore increases the induction time. The competition between these reactions, and the consequent distribution of fast O, H and OH radicals and the slow radical HO_2, is strongly temperature dependent. Z22 includes reactions important for the complete temperature spectrum, below and above the crossover region. In the mechanism development, particular efforts were spent on improving its capability to match the ignition experimental behaviour also in the intermediate connecting region, because it is extremely useful for ensuring flame anchoring and stabilization within the supersonic combustion engines. At low temperatures, reaction [R12] predominates over the reaction [R4], the HO_2 concentration enhances and new reaction paths become more important i.e., [R16]:

[R16] $HO_2 + HO_2 \rightarrow H_2O_2 + O_2$

and [R20]:

[R20] $H_2O + HO_2 \rightarrow H_2O_2 + OH$

These reactions increase the concentration of H_2O_2, which main consumption route is carried out by means of reaction [R17]:

[R17] $H_2O_2\ (+M) \rightarrow OH + OH\ (+M)$

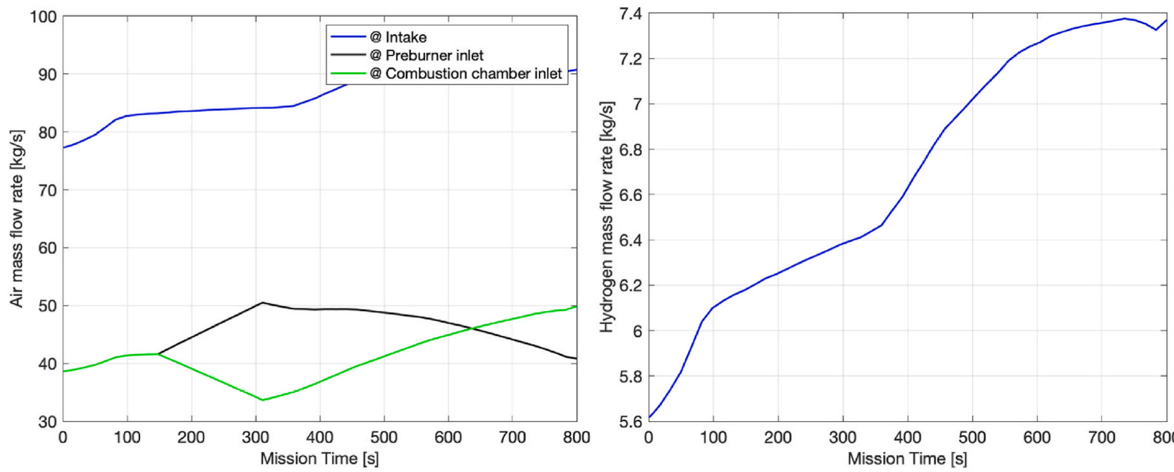

Fig. 7. a) Variation of air mass flow rate along the trajectory at different stations of the engine; b) variation of hydrogen mass flow rate along the mission.

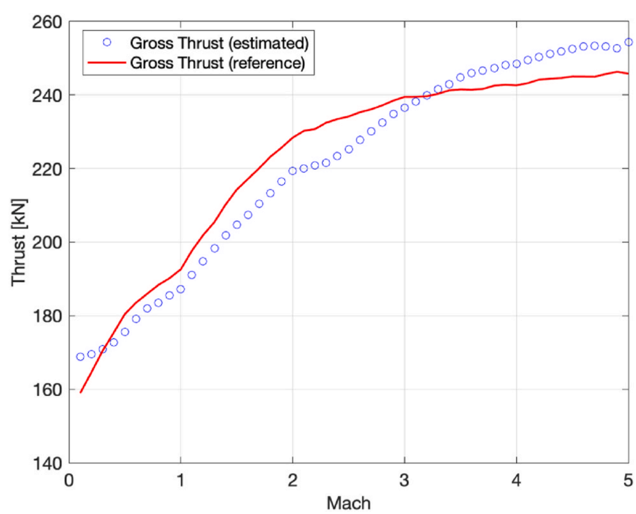

Fig. 8. Comparison of the estimated thrust output for ¼ of SABRE and the reference thrust profile available in Ref. [29].

which produces two OH radicals, which in turn generates H radical through [R8]:

[R8] $H_2 + OH \rightarrow H_2O + H$

The improvement consists of the addition of the following two pressure-dependent irreversible reactions for the production of the fundamental OH radical:

[R23] $H_2O_2 + N_2 \rightarrow OH + OH + N_2$

[R24] $H_2O_2 + O_2 \rightarrow OH + OH + O_2$

The 0D simulations of the preburner combustion were carried out in isobaric conditions, while the simulations for the combustion chamber were performed under isochoric assumptions. Moreover, the composition of the exhaust gases exiting the preburner was used as input for the combustion chamber after mixing with the additional air stream coming from the intake. In this way, a chemical kinetic Emission Inventory was built to be compared with the EINOx predicted by the P3-T3 method.

4.2.1. Application to the SABRE engine

In order to build the emissive database of the SABRE engine operating in air-breathing mode, the detailed outputs of the propulsive model built in Section 4.1 have been used. In detail, in order to initialize the 0D chemical-kinetic simulations with Cantera software tools, the following set of input data were necessary: atmospheric air pressure at the entrance of the preburner (station 4) as well as after the preburner

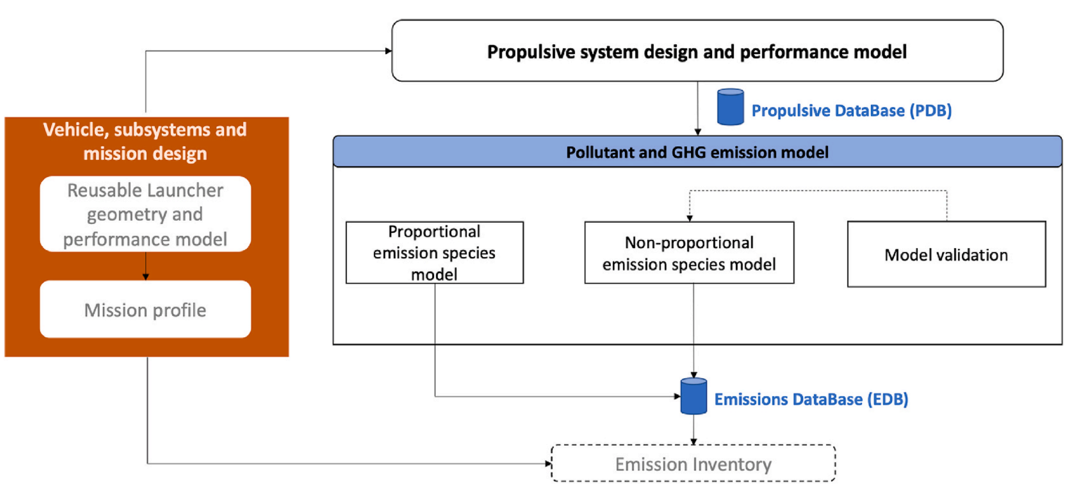

Fig. 9. Chemical Emissions estimation activity flow.

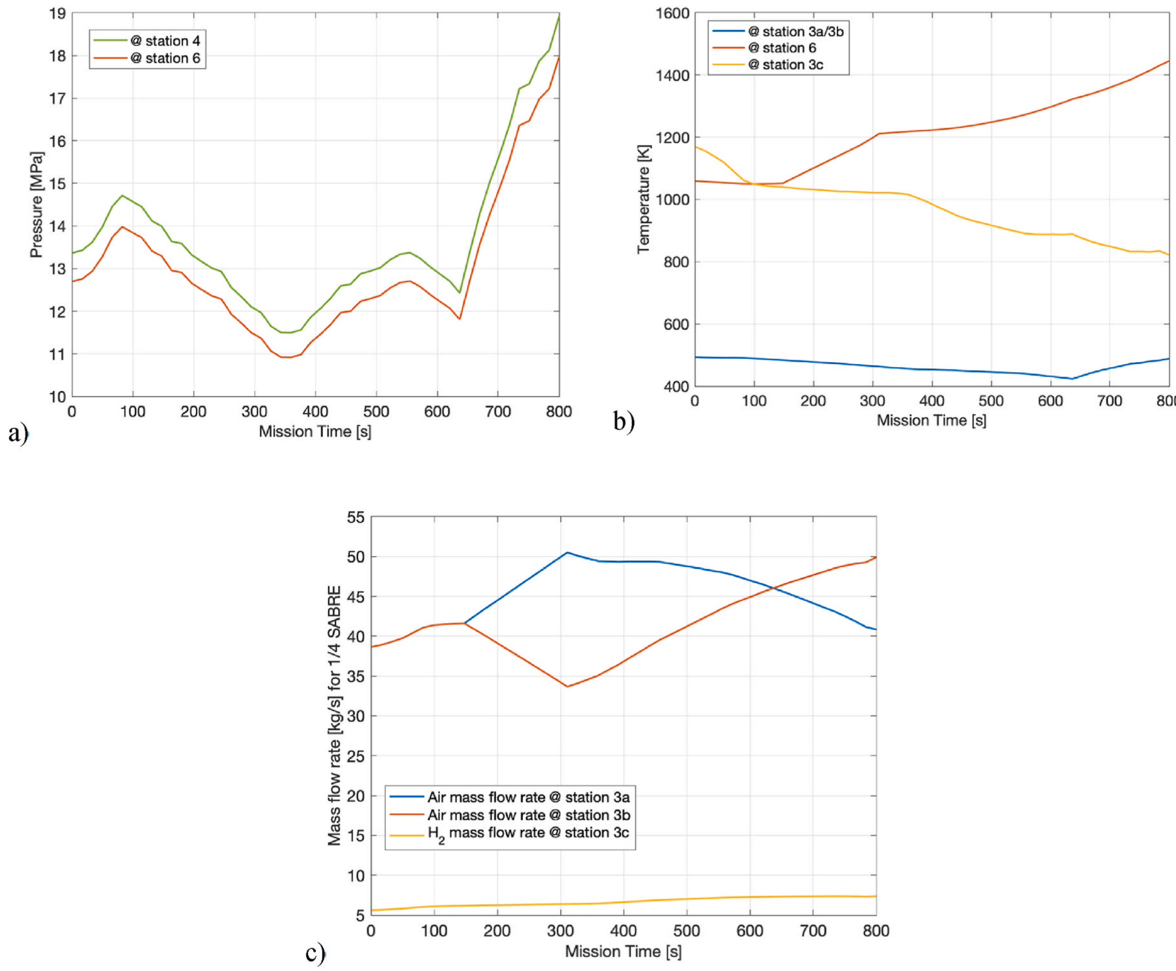

Fig. 10. Input data for the 0D-chemical kinetic simulations in Cantera: a) pressure, b) temperature, c) mass flow rate variation along the trajectory at different stations of the engine thermodynamic cycle.

exhaust-helium heat exchanger (station 6), as reported in Fig. 10a; atmospheric air temperature after the compressor stage (*station 3a* and *3b*), after the preburner exhaust-helium heat exchanger (*station 6*) as well as the hydrogen temperature when injected in the preburner mixer (*station 3c*), as reported in Fig. 10b; and the mass flow rate of the air entering the preburner (*station 3a*) and the combustion chamber (*station 3b*) together with the hydrogen flow rate injected in the preburner (*station 3c*), as reported in Fig. 10c.

The main results of the Cantera simulation for the SABRE engine are reported in Table 2.

A proper validation using different chemical-kinetic mechanisms to predict EINO values is not possible due to their inferior performance, thus preventing from a meaningful direct comparison of the results. A clear example can be provided by CRECK-NOx [42–44], which may fail

Table 2
Main output of the 0D chemical kinetic simulations in Cantera.

	Flame Temperature [K]	Ignition delay time [μs]	NO mass fraction	H_2 mass fraction	H_2 injection mass fraction	EINO [gNO/kg H_2 burnt]
M = 0.1	1956	396	2,50E-05	0,036	0,050	**1804**
M = 0.2	1955	401	2,48E-05	0,036	0,050	**1791**
M = 0.3	1954	402	2,48E-05	0,036	0,050	**1791**
M = 0.4	1952	406	2,47E-05	0,036	0,050	**1779**
M = 0.5	1952	399	2,48E-05	0,036	0,050	**1786**
M = 0.6	1950	406	2,43E-05	0,036	0,050	**1754**
M = 0.7	1950	409	2,43E-05	0,036	0,050	**1753**
M = 0.8	1950	413	2,42E-05	0,036	0,050	**1746**
M = 0.9	1890	390	9,87E-06	0,046	0,060	**0,712**
M = 1	1890	394	9,84E-06	0,046	0,060	**0,710**
M = 1.5	1863	126	6,77E-06	0,047	0,060	**0,537**
M = 2	1889	48	9,71E-06	0,039	0,050	**0,857**
M = 2.5	1846	45	4,97E-06	0,049	0,060	**0,438**
M = 3	1916	40	1,17E-05	0,045	0,057	**0,965**
M = 3.5	1964	31	2,08E-05	0,046	0,059	**1638**
M = 4	2034	23	4,83E-05	0,047	0,060	**3586**
M = 4.5	2094	12	1,10E-04	0,047	0,061	**7785**
M = 5	2187	5	3,28E-04	0,048	0,063	**22,214**

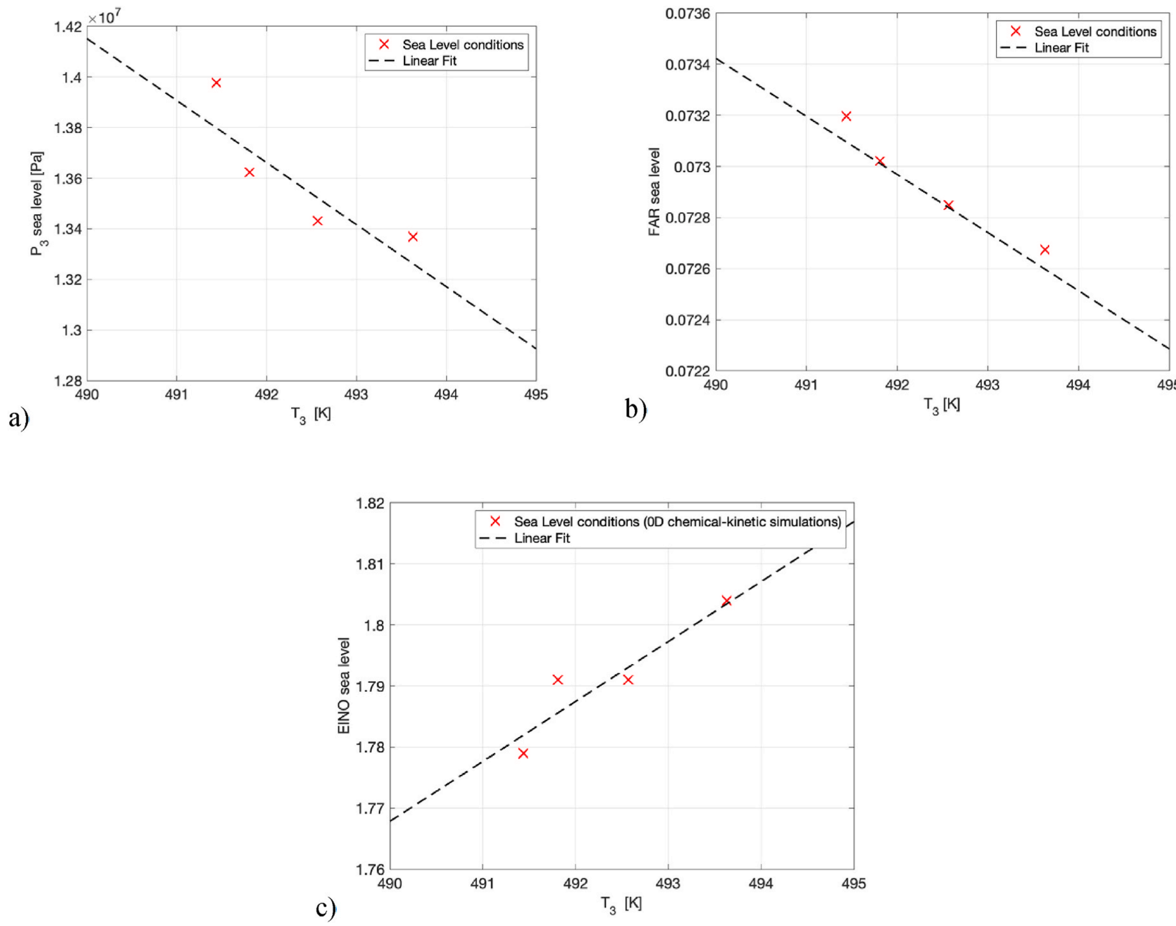

Fig. 11. Sea level conditions, in terms of a) pressure at the inlet of the combustion chamber, b) Fuel to air ratio and c) EINO as a function of the combustion inlet temperature.

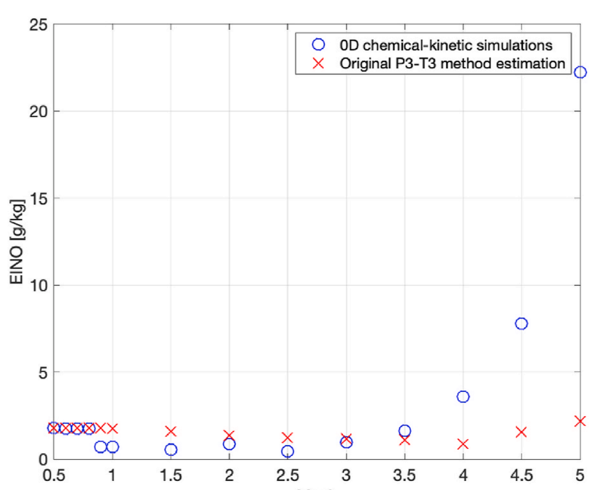

Fig. 12. Nitrogen Oxides emission indices estimations with the original (red crosses) P_3T_3 method (green and black crosses) throughout the entire Mach number profile compared to the results of the 0D chemical-kinetic simulations.

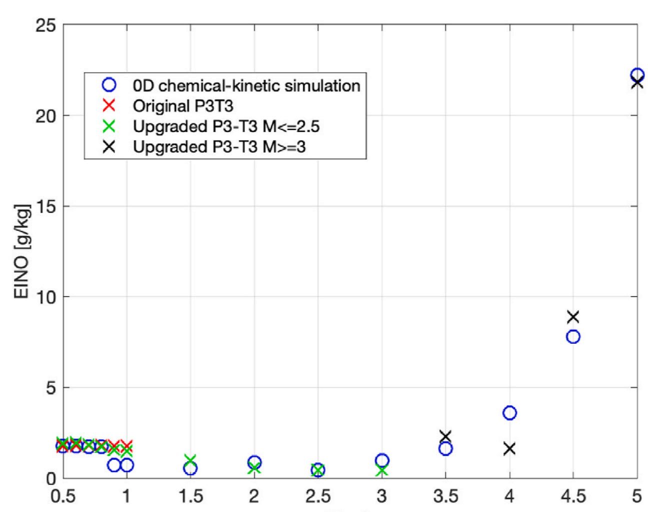

Fig. 13. Nitrogen Oxides emission indices estimations with the original (red crosses) and the upgraded P_3T_3 method (green and black crosses) compared to the results of the 0D chemical-kinetic simulations.

in providing accurate results at pressure higher than 100 bars, as for the SABRE's main combustion chamber.

However, the average resulting nitrogen oxides emission index is well in line with the value of 14 g/kg reported in Ref. [25]. It is worth remembering that the NOx estimation model used in that publication is purely based on a stochiometric reaction, neglecting initialization, branching, chain propagation and termination mechanisms which have been experimentally demonstrated to be highly important for the correct prediction of NOx formation in H_2-air combustion process [26].

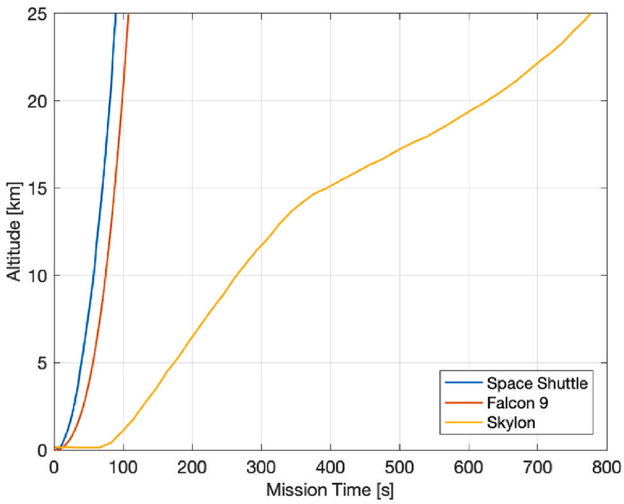

Fig. 14. Comparison of the ascent profiles (up to 25 km) of Space Shuttle, Falcon 9 and Skylon.

4.3. Upgraded P3-T3 formulation

The third part of the methodology consists of the final upgrade of the P_3-T_3 method to extend its applicability to high-speed engines using non-conventional fuels.

At first, the propulsive model and the emissive database have been used to generate and analyse the sea level conditions as graphically reported in Fig. 11.

For the SABRE engine, reference sea level conditions as function of the combustor (preburner) inlet temperature can be mathematically expressed with the following equations:

$$P_{3SL} = -2.452 \bullet 10^5 \bullet T_3 + 1.343 \bullet 10^8 \tag{2}$$

$$FAR_{SL} = -2.273 \bullet 10^{-4} \bullet T_3 + 0.185 \tag{3}$$

$$EINO_{SL} = 9.81 \bullet 10^{-3} \bullet T_3 - 3.043 \tag{4}$$

Using the FL conditions estimated with the propulsive models and benefitting from the trends in Eqs. (2)–(4), the original formulation of the method (Eq. (1)) is applicable below Mach 0.9. As clearly visible in Fig. 12, starting from the transonic speed regime, new phenomena occur in the combustion process and nitrogen oxides formation, which shall be captured by different exponents or variables in the formulation.

Benefitting from the 0D chemical-kinetic simulations results, the P_3-T_3 method has been upgraded as reported in the following equation.

$$EINO_{x_{FL}} = EINO_{xSL}\left(\frac{P_{3FL}}{P_{3_{SL}}}\right)^a \left(\frac{FAR_{FL}}{FAR_{SL}}\right)^b e^H \ where \begin{cases} a = 1.97; b = 0 & for\ Mach \leq 2.5 \\ a = -5; b = 39 & for\ Mach \geq 3 \end{cases} \tag{5}$$

Looking at the subsonic and low supersonic speed regime, the $\left(\frac{P_{3FL}}{P_{3SL}}\right)$ ratio ranges from 1.05 to 0.7, while the $\left(\frac{FAR_{FL}}{FAR_{SL}}\right)$ ratio varies from 1.005 to 0.975, thus showing a variation which is two orders of magnitude lower than the pressure ratio. On one side, this justifies the indication of the original method to keep the exponent of the FAR ratio equal to zero, while on the other hand, the FAR ratio appears to be negligible up the low supersonic speed regime, for Mach lower than 2.5. From the mathematical standpoint, it can be observed that the $\left(\frac{P_{3FL}}{P_{3SL}}\right)$ ratio is proportional $\left(\frac{EINO_{FL}}{EINO_{SL}}\right)$ ratio, which implies a positive a exponent. This is fully justified from the chemical-physical point of view, considering that a decrease of pressure at the entrance of the combustion chamber (decreasing trend of $\left(\frac{P_{3FL}}{P_{3SL}}\right)$ ratio reported in this speed regime) results in a lower flame temperature, leading to a reduction of NOx emissions (decreasing trend of $\left(\frac{EINO_{FL}}{EINO_{SL}}\right)$ ratio).

Looking at the high-supersonic and hypersonic speed regime, the $\left(\frac{P_{3FL}}{P_{3SL}}\right)$ ratio and $\left(\frac{FAR_{FL}}{FAR_{SL}}\right)$ ratio variations become closer and respectively equal to 0.4 and 0.06. Therefore, the contribution of the fuel to air ratio cannot be neglected anymore. In particular, SABRE operates in fuel-rich conditions, where a reduction of NOx can be achieved only through an increase in FAR. Therefore, the FAR ratio decreasing trend moves the engine operating point closer to the stochiometric condition, where the NOx pick value is achieved. A graphical comparison of the original and novel formulations is reported in Fig. 13. The novel formulation which extends the applicability of the P3-T3 method to hydrogen fuelled engines and supersonic and hypersonic speed regimes well fits the emission data from the 0D chemical-kinetic simulations.

Table 3
Space Shuttle, Falcon 9 and Skylon comparison.

	Space Shuttle	Falcon 9	Skylon
Type of propellant	*SSME*: LOX/ Hydrogen *RSRM*: APCP (PBAN)	LOX/RP-1	Hydrogen
Propellant burnt up to 25 km [kg]	860,000	310,000	42,783
Payload in LEO [kg]	25,000	22,900	15,000
CO_2 up to 25 km [kg]	30,1516	29,1257	0
CO up to 25 km [kg]	1041	1076	0
H_2O up to 25 km [kg]	366,271	116,950	376,490
Cl_x up to 25 km [kg]	157,946	0	0
Al_2O_3 up to 25 km [kg]	221,125	0	0
NO_x up to 25 km [kg]	9533	4183	68
BC up to 25 km [kg]	908	373	0

5. Results

Thanks to the methodology presented in the previous sections, it is possible to estimate the nitrogen oxides production of the Skylon throughout its air-breathing ascending trajectory and to compare it with the emissions produced by the first stage of traditional rocket-based space launchers. For the sake of fairness, Skylon's trajectory has been compared to the Space Shuttle and Falcon 9 ascents up to 25 km (Fig. 14). Space Shuttle and Falcon 9 NOx productions have been estimated thanks to data available from Ref. [14] coupled with simulations performed with RUMBLE 3.0, a Blue Ridge Research and Consulting integrated tool that enables practitioners to accurately model the noise and emissions produced by commercial space vehicles. The commercial space vehicle emissions model of RUMBLE 3.0 is based on the best publicly available data in the literature. However, it contains uncertainty due to the scarcity of high-quality emissions data. The emissions model of the Space Shuttle has been validated thanks to the well-documented emissions legacy data and therefore, it has been selected for this comparison.

Table 3 reports the dataset used to compare the different concepts. It

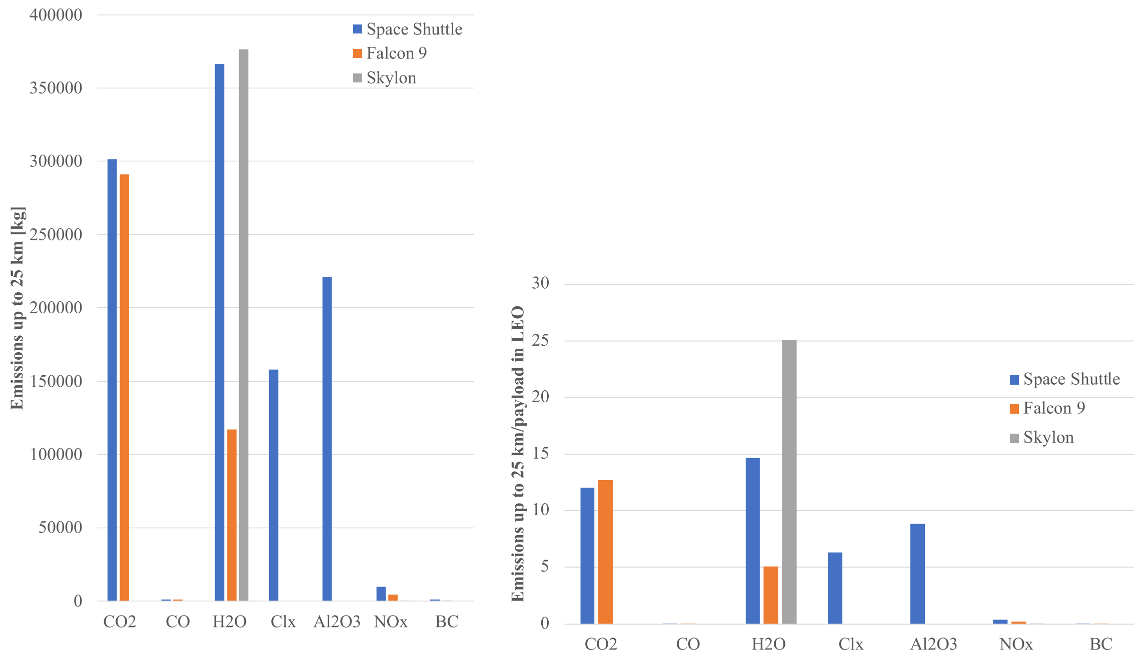

Fig. 15. Comparison of chemical emissions produced up to 25 km by Space Shuttle, Falcon 9 and Skylon in terms of overall amount by species and b) relative emissions (kg emissions/kg fuel burnt) by species.

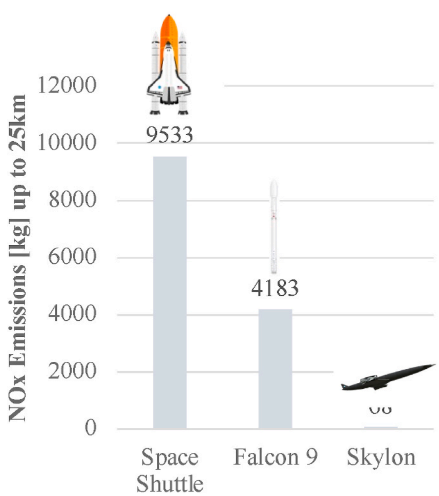

Fig. 16. Comparison of nitrogen oxides emissions up to 25 km.

is worth noting that the three concepts (i.e. Space Shuttle, Falcon 9 and Skylon) make use of different types of liquid propellant, with a direct impact on the chemical species emitted during the combustion process as reported in Fig. 15. It is evident that one of the main advantages of hydrogen-fuelled air-breathing launchers from the environmental perspective is the production of nitrogen oxides and water vapour only, getting rid of carbon-related emissions (CO, CO_2, BC) and any other chemical species including chlorine and alumina. However, comparing the amount of species emitted per kg of payload delivered in LEO, Skylon appears as the greatest contributor to water vapour emission. This is due to the chemistry of the air and hydrogen combustion, thus it cannot be avoided. However, many scientists are trying to better predict the climate perturbation caused by the introduction of hydrogen as a propellant at different altitudes [41–43,45–49]. Finally, a comparison in terms of nitrogen oxides emissions is presented (Fig. 161). Along its reference trajectory, Skylon produces 68 kg of nitrogen oxides, three orders of magnitude lower than the analyzed competitors. On one side, this is due to the lower $EINO_x$ (about 33 g/kg for Space Shuttle and Falcon 9 at sea level and only 2 g/kg for the Skylon in the same conditions) and on the other side to the lower fuel consumption (about 4500 kg/s for Space Shuttle, 319 kg/s for Falcon 9 and 40 kg/s for Skylon).

The results of the 0D chemical-kinetic simulations are usually strongly affected by the initial conditions in terms of pressure and temperature. However, in this specific case, the pressure levels at the beginning of the combustion process are very high (around 120–130 bar), thus ensuring that all considered operating points are above the third explosion limit of the hydrogen-air explosivity diagram [50]. In this operating region, small uncertainties in pressure and temperature estimation are expected to have negligible effects onto the final emissions estimation. In addition, the emission indexes disclosed in this paper are in very good agreement with the stoichiometric values reported by Larson.

6. Conclusions

This paper discloses an integrated methodology to complement conceptual design of new launchers with emissions estimations. Specifically, it provides useful guidelines for the estimation of nitrogen oxides emissions for a hydrogen-fuelled air-breathing concept. The proposed strategy combines multi-fidelity propulsive system modelling with 0D chemical-kinetic air/hydrogen combustion numerical simulations to define high-fidelity emissive database representative of various on-ground and in-flight operative conditions. The propulsive and emissive databases are then used to develop and unveil a new analytical formulation able to predict nitrogen oxides emission indices in any in-flight conditions, perfectly fitting the conceptual design needs. Throughout the paper, the Skylon spaceplane and its Synergetic Air Breathing Rocket Engine are used as reference case study.

Main findings and conclusions can be summarized as follows.

1. The paper highlights the need to develop and implement holistic design methodologies to support the design of future sustainable space launchers. The variety of airframe configurations, propulsive

technologies, propellants, and operational strategy impose to extend the current multidisciplinary approaches towards holistic design methodologies embracing environmental, economic, and technological sustainability assessments.

2. The methodology allows proving the high competitiveness of air-breathing space launchers with respect to well-known past and current competitors, by predicting nitrogen oxides for the reusable air-breathing concept, which are three orders of magnitude lower than the analyzed competitors, i.e. Space Shuttle and Falcon 9. In addition, the combination of the methodology described in this paper with Life Cycle cost estimation and Technology Roadmapping [51] can provide a complete and exhaustive environmental-economical-technological assessment of the sustainability of future reusable launchers.
3. The P_3T_3 method, originally developed for civil subsonic aviation, has proved to be still applicable to predict the performance of the SABRE engine when operating in subsonic mode.
4. However, a variation of the exponents of the formulation is sufficient to extend the applicability of the original P3T3 method beyond the transonic regime, up to Mach 5, thus unveiling an upgraded P_3T_3 method, i.e. the H2–P_3T_3 method. The H2–P_3T_3 method is a new analytical formulation that applies to air-breathing engines that operates with hydrogen up to Mach 5. The H2–P_3T_3 method provides the basis to develop analytical formulations able to capture the basic chemical-physical phenomena of hydrogen combustion.

This work opens different ways forward including.

1. The upgrade of the high-fidelity emission database with 1D chemical-kinetic simulations 0 of the entire SABRE engine (not just ¼ of it), taking into account shock formations inside the engines and mixing effects at the outlet of the four thrust chamber nozzles.
2. The upgrade of the SABRE modelling by including an accurate model of the entire helium cycle. This will guarantee the possibility to predict the evolution of the helium's physical properties throughout the cycle and understand the related impact on the final engine performance, including the emission index.
3. To the authors' knowledge, there are no available emission experimental data of the SABRE engine to allow a proper validation. However, the authors are currently cooperating with REL in the framework of the H2020 MORE&LESS Project (https://doi.org/10.3030/101006856), where higher fidelity data is expected to be delivered soon. Benefitting of a multi-fidelity approach in which experimental combustion test campaigns with exhausts measurement are used to validate Large Eddy Simulations, which can then be used to validate the 0D/1D chemical/kinetic simulations performed using Cantera.
4. The validation of H2–P_3T_3 method against a new data set, following the same workflow reported in Section 4 but for different Mach numbers.
5. The upgrade of other mathematical formulations, such as the Fuel Flow Method [52,53] to improve the conceptual design phase of reusable launchers.
6. The application of the methodology disclosed in this paper to other reusable access to space vehicles design. This attempt might include the possibility of checking the capability of the STRATOFLY MR3 hypersonic civil passenger cruiser [54] to act as first stage of a reusable access to space vehicle.
7. The upgrade of the holistic methodology coupling the emission estimation models with atmospheric and climate impact models to capture predict actual environmental impact of the introduction of a new space launcher.

Declaration of competing interest

The authors declare that they have no known competing financial interests or personal relationships that could have appeared to influence the work reported in this paper.

Acknowledgment

The authors wish to sincerely thank Giovanni Grimaldi for starting the development of the SABRE propulsive model during his MSc. Thesis at Politecnico di Torino.

References

[1] Stanley Morgan, *Space: Investing In the Final Frontier*. Morgan Stanley, 2020. Retrieved form Retrieved from, https://www.morganstanley.com/. ideas/investing-in-space.
[2] https://www.morganstanley.com/ideas/space-economy-investment-themes.
[3] E. Sirieys, C. Gentgen, A. Jain, J. Milton, O.L. de Weck, Space sustainability isn't just about space debris: on the atmospheric impact of space launches, MIT Science Policy Review 3 (2022) 143–151, https://doi.org/10.38105/spr.whfig18hta.
[4] L. Miraux, A. Ross Wilson, G.J.D. Calabuig, Environmental sustainability of future proposed space activities, Acta Astronaut. 200 (2022) 329–346, https://doi.org/10.1016/j.actaastro.2022.07.034. ISSN 0094-5765.
[5] M.N. Ross, P.M. Sheaffer, Radiative forcing caused by rocket engine emissions, Earth's Future 2 (2014) 177–196, https://doi.org/10.1002/2013EF000160.
[6] F. Simmons, Rocket Exhaust Plume Phenomenology, The Aerospace Press, El Segundo, Calif, 2000 chap. 9.
[7] L. Wilcox, K. Shine, B. Hoskins, Radiative forcing due to aviation water vapor emissions, Atmos. Environ. 63 (2012) 1–13.
[8] J. Pletzer, D. Hauglustaine, Y. Cohen, P. Jöckel, V. Grewe, The climate impact of hydrogen-powered hypersonic transport, Atmos. Chem. Phys. 22 (21) (2022) 14323–14354, https://doi.org/10.5194/acp-22-14323-2022.
[9] D. Waugh, T. Hall, Age of stratospheric air: theory, observations and models, Rev. Geophys. 40 (2002) 4, https://doi.org/10.1029/2000RG000101.
[10] J.H. Seinfeld, S.N. Pandis, Atmospheric Chemistry and Physics: from Air Pollution to Climate Change, 3rd, Wiley, 2016.
[11] J.A. Dallas, S. Raval, J.P. Alvarez Gaitan, S. Saydam, A.G. Dempster, The environmental impact of emissions from space launches: a comprehensive review, J. Clean. Prod. 255 (2020) 120209, https://doi.org/10.1016/j.jclepro.2020.120209. ISSN 0959-6526.
[12] N. Viola, R. Fusaro, D. Ferretto, V. Vercella, Research, development and production costs prediction parametric model for future civil hypersonic aircraft, Acta Astronaut. 204 (2023) 58–72, https://doi.org/10.1016/j.actaastro.2022.12.036.
[13] N. Viola, R. Fusaro, V. Vercella, Technology roadmapping methodology for future hypersonic transportation systems, Acta Astronaut. 195 (2022) 430–444, https://doi.org/10.1016/j.actaastro.2022.03.038.
[14] National Academies of Sciences, Engineering, and Medicine, Commercial Space Vehicle Emissions Modeling, The National Academies Press, Washington, DC, 2021, https://doi.org/10.17226/26142.
[15] H.S. Pergament, R.I. Gomberg, I.G. Poppoff, NOx deposition in the stratosphere from the space Shuttle rocket motors, in: A.E. Potter (Ed.), Proceedings of the Space Shuttle Environmental Assessment Workshop on Stratospheric Effects, National Aeronautics and Space Administration, Houston, Texas, 1977.
[16] H.S. Pergament, R.D. Thorpe, NOx Deposited in the Stratosphere by the Space Shuttle. Final Summary Report: Phase I, National Aeronautics and Space Administration, 1975. CR-132715.
[17] H.S. Pergament, R.D. Thorpe, B. Hwang, NOx Deposited in the Stratosphere by the Space Shuttle Solid Rocket Motors, National Aeronautics and Space Administration, CR, 1975 144928.
[18] Environmental Impact Statement for the Space Shuttle Program, National Aeronautics and Space Administration, Washington, D.C., 1978.
[19] R.I. Gomberg, R.B. Stewart, A Computer Simulation of the Afterburning Processes Occurring within Solid Rocket Motor Plumes in the Troposphere, National Aeronautics and Space Administration, Washington, D.C., 1976.
[20] Final Environmental Impact Statement Space Shuttle Advanced Solid Rocket Motor Program, National Aeronautics and Space Administration, Washington, D.C., 1989.
[21] Environmental Impact Statement for Advanced Solid Rocket Motor Testing at Stennis Space Center, National Aeronautics and Space Administration, TM-, August 1990 107818.
[22] D.M. Leone, S.R. Turns, Active Chlorine and Nitric Oxide Formation from Chemical Rocket Plume Afterburning, National Aeronautics and Space Administration, CR, 1994 197503.
[23] M.R. Denison, J.J. Lamb, W.D. Bjorndahl, E.Y. Wong, P.D. Lohn, Solid rocket exhaust in the stratosphere - plume diffusion and chemical reactions, J. Spacecraft Rockets 31 (3) (1994) 435–442, https://doi.org/10.2514/3.26457.
[24] P.F. Zittel, Computer model predictions of the local effects of Large, solid-fuel rocket motors on stratospheric ozone, in: Space and Missile Systems Center, Los Angeles Air Force Base, 1994. California, SMC-TR-94-36.
[25] E.J.L. Larson, R.W. Portmann, K.H. Rosenlof, D.W. Fahey, J.S. Daniel, M.N. Ross, Global atmospheric response to emissions from a proposed reusable space launch system, Earth's Future 5 (2017) 37–48, https://doi.org/10.1002/2016EF000399.
[26] Y. Zhang, O. Mathiu, E.L. Petersen, G. Bourque, J.H. Curran, Assessing the prediction of a NOx kinetic mechanism on recent hydrogen and syngas experimental data, Combust. Flame 182 (2017), https://doi.org/10.1016/j.combustflame.2017.03.019, 122.

[27] N. Chandrasekaran, A. Guha, Study of prediction methods for NOx emission from turbofan engines, J. Propul. Power 28 (2012) 170–180, https://doi.org/10.2514/1.B34245, 1.
[28] I.C.A.O. Icao, Annex 16 Volume II Aircraft Engine Emissions, ICAO, Montreal, Canada, 2014.
[29] V. Fernández Villacé, Simulation, Design and Analysis of Air-Breathing Combined-Cycle Engines for High Speed Propulsion, Diss. Aeronauticos, 2013.
[30] H. Kobayashi, T. Sato, H. Taguchi, K. Fujita, S. Sawai, N. Tanatsugu, T. Kojima, K. Okai, Y. Maru, Development status of mach 6 turbojet engine in JAXA, International Astronautical Federation - 55th International Astronautical Congress 11 (2004) 7129–7135, 2004.
[31] T. Sato, N. Tanatsugu, Y. Naruo, J. Omi, J. Tomike, T. Nishino, Development study on ATREX engine, Acta Astronaut. 47 (11) (2000) 799–808, https://doi.org/10.1016/S0094-5765(00)00129-6.
[32] T. Sato, H. Taguchi, H. Kobayashi, T. Kojima, K. Fukiba, D.M.K. Okai, K. Fujita, M. Hongo, S. Sawai, Development study of a precooled turbojet engine, Acta Astronaut. 66 (7–8) (2010) 1169–1176, https://doi.org/10.1016/j.actaastro.2009.10.006.
[33] M. Hempsell, R.A. Logstaff, Bond. Skylon Users' Manual, Reaction Engines Ltd. , Fulham Science Centre, United Kingdom, 2010.
[34] R. Varvill, A. Bond, The Skyline spaceplane: progress to realisation, J. Br. Interplanet. Soc. (JBIS) (2008).
[35] J. Zhang, Z. Wang, Q. Li, Thermodynamic efficiency analysis and cycle optimization of deeply precooled combined cycle engine in the air-breathing mode, Acta Astronaut. 138 (Sep. 2017) 394–406, https://doi.org/10.1016/J.ACTAASTRO.2017.06.011.
[36] https://space.stackexchange.com/questions/12545/why-is-the-sabre-engine-curved. Accessed online on the 1st of August 2023.
[37] J.D. Mattingly, W.H. Heiser, D.T. Pratt, Aircraft Engine Design, second ed., Jan. 2002, https://doi.org/10.2514/4.861444 eISBN: 978-1-60086-144-4.
[38] G. Saccone, A.C. Ispir, B.H. Saracoglu, L. Cutrone, M. Marini, Computational evaluations of emissions indexes released by the STRATOFLY air-breathing combined propulsive system, Aircraft Eng. Aero. Technol. (2022), https://doi.org/10.1108/AEAT-01-2022-0024/FULL/PDF ahead-of-print, no. ahead-of-print.
[39] D. Goodwin, H.K. Moffat, R.L. Speth, Cantera: an Object-Oriented Software Toolkit for Chemical Kinetics, Thermodynamics, and Transport Processes, 2023.) [Online]. Available:, Version 2.6. http://www.cantera.org.
[40] N. Zettervall, C. Fureby, Computational study of ramjet, scramjet and dual mode ramjet/scramjet combustion in a combustor with a cavity flameholder, in: Proceedings of AIAA Aerospace Science, Meeting Kissimmee, Florida, 8-12 January 2018. U.S.A.).
[41] N. Zettervall, Reaction Mechanism for Hydrogen-Air Combustion, FOI-D-1153-SE, 2022.
[42] N.A. Cuoci, A. Frassoldati, T. Faravelli, E. Ranzi, OpenSMOKE++: an object-oriented framework for the numerical modeling of reactive systems with detailed kinetic mechanisms, Comput. Phys. Commun. 192 (Jul. 2015) 237–264, https://doi.org/10.1016/J.CPC.2015.02.014.
[43] A. Frassoldati, T. Faravelli, E. Ranzi, A wide range modeling study of NOx formation and nitrogen chemistry in hydrogen combustion, Int. J. Hydrogen Energy 31 (15) (Dec. 2006) 2310–2328, https://doi.org/10.1016/J.IJHYDENE.2006.02.014.
[44] E. Ranzi, et al., Hierarchical and comparative kinetic modeling of laminar flame speeds of hydrocarbon and oxygenated fuels, Prog. Energy Combust. Sci. 38 (4) (Aug. 2012) 468–501, https://doi.org/10.1016/J.PECS.2012.03.004.
[45] IPCC, in: J.E. Penner, D.H. Lister, D.J. Griggs, D.J. Dokken, M. McFarland (Eds.), Special Report on Aviation and the Global Atmosphere, Intergovernmental Panel on Climate Change, Cambridge University Press, New York, NY, USA, 1999.
[46] V. Grewe, A. Stenke, M. Ponater, R. Sausen, G. Pitari, D. Iachetti, H. Rogers, O. Dessens, J. Pyle, I.S.A. Isaksen, L. Gulstad, O.A. Søvde, C. Marizy, E. Pascuillo, Climate impact of supersonic air traffic: an approach to optimize a potential future supersonic fleet - results from the EU-project SCENIC, Atmosphere Chemistry and Physics (7) (2007) 5129–5145, https://doi.org/10.5194/acpd-7-6143-2007.
[47] V. Grewe, Climate Impact Hypersonic Aviation, von Karman Institute Lecture Series, Lecture Series, May 2021, pp. 25–27.
[48] N. Viola, R. Fusaro, D. Ferretto, O. Gori, B. Saracoglu, A.C. Ispir, C. Schram, V. Grewe, J.F. Plezer, J. Martinez, M. Marini, L. Cutrone, G. Saccone, S. Hernandez, K. Lammers, A. Vincent, D. Hauglustaine, B. Liebhardt, F. Linke, D. Bodmer, T. Nilsson, C. Fureby, C. Ibron, H2020 STRATOFLY PROJECT: FROM EUROPE TO AUSTRALIA IN LESS THAN 3 HOURS (2021) 32nd Congress of the International Council of the Aeronautical Sciences, 2021. ICAS.
[49] J. Pletzer, D. Hauglustaine, Y. Cohen, P. Jöckel, V. Grewe, The climate impact of hydrogen-powered hypersonic transport, Atmos. Chem. Phys. 22 (21) (2022) 14323–14354, https://doi.org/10.5194/acp-22-14323-2022.
[50] N. Viola, R. Fusaro, G. Saccone, V. Borio, Analytical formulations for nitrogen oxides emissions estimation of an air turbo-rocket engine using hydrogen, Aerospace 10 (2023) 909, https://doi.org/10.3390/aerospace10110909.
[51] M.A. Viscio, E. Gargioli, J.A. Hoffman, P. Maggiore, A. Messidoro, N. Viola, Future space exploration: from reference scenario definition to key technologies roadmaps, Proceedings of the International Astronautical Congress, IAC 11 (2012) 9131–9145.
[52] R. Fusaro, N. Viola, D. Galassini, Sustainable supersonic fuel flow method: an evolution of the boeing fuel flow method for supersonic aircraft using sustainable aviation fuels, Aerospace 8 (2021) 331, https://doi.org/10.3390/aerospace8110331.
[53] D. DuBois, G.C. Paynter, Fuel flow Method 2 for estimating aircraft emissions, SAE Trans. 115 (2006) 1–14.
[54] N. Viola, R. Fusaro, O. Gori, M. Marini, P. Roncioni, G. Saccone, B. Saracoglu, A. C. Ispir, C. Fureby, T. Nilsson, C. Ibron, N. Zettervall, K.N. Bates, A. Vincent, J. Martinez-Schram, V. Grewe, J. Pletzer, D. Hauglustaine, F. Linke, D. Bodmer, Stratofly mr3 – how to reduce the environmental impact of high-speed transportation, AIAA Scitech 2021 Forum (2021) 1–21. Saccone, G., Natale, P., Cutrone, L., Marini, M., Hydrogen/Air Supersonic Combustion Modelling and Validation for Scramjet Applications, Journal of Fluid Flow, . 9 (2022) DOI: 10.11159/jffhmt.2022.017.